AIP | Journal of Applied Physics

Forming-free resistive switching behaviors in Cr-embedded Ga2O3 thin film memories

Dai-Ying Lee and Tseung-Yuen Tseng

Citation: Journal of Applied Physics **110**, 114117 (2011); doi: 10.1063/1.3665871
View online: http://dx.doi.org/10.1063/1.3665871
View Table of Contents: http://scitation.aip.org/content/aip/journal/jap/110/11?ver=pdfcov
Published by the AIP Publishing

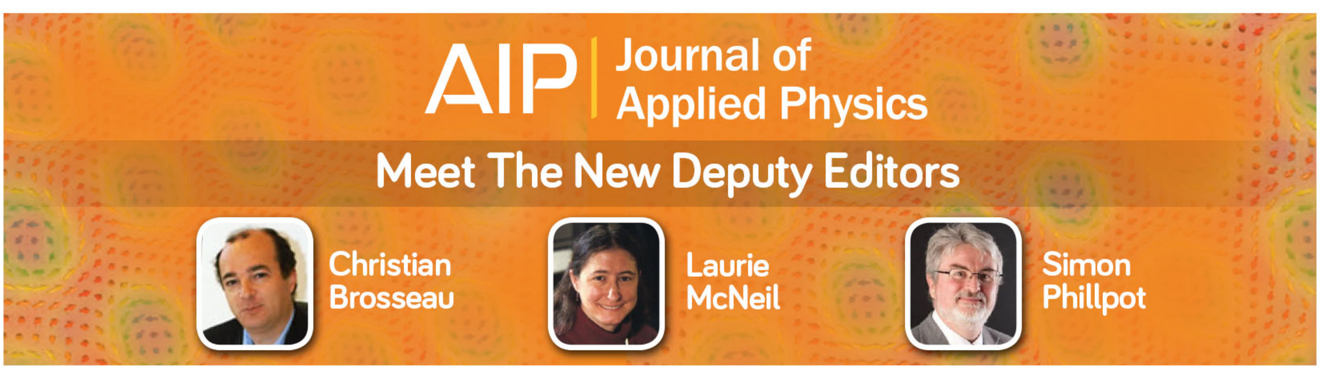

JOURNAL OF APPLIED PHYSICS 110, 114117 (2011)

Forming-free resistive switching behaviors in Cr-embedded Ga_2O_3 thin film memories

Dai-Ying Lee and Tseung-Yuen Tseng[a)]
Department of Electronics Engineering and Institute of Electronics, National Chiao Tung University, Hsinchu 300, Taiwan

(Received 23 August 2011; accepted 4 November 2011; published online 9 December 2011)

Resistive switching behaviors are studied for the rapid thermal annealing (RTA) Ga_2O_3 thin film embedding a Cr metal layer. By modifying the thickness, area, and RTA temperature of the device, the thermal-induced resistive switching is similar to those induced by the electrical forming process. The conducting filaments composed of oxygen vacancies are created by the Cr diffusion and oxidization during RTA. The related carrier conduction mechanism obeys space charge limited conduction theory accompanied by the formation/rupture of the conducting filaments at the interface between Ti and Cr:Ga_2O_3 film. This study demonstrates a convenient process to fabricate forming-free resistive switching memory devices. © *2011 American Institute of Physics*. [doi:10.1063/1.3665871]

I. INTRODUCTION

In recent years, gallium oxide (Ga_2O_3) has been extensively investigated for use in luminescent phosphor, high-temperature oxygen sensor, deep-ultraviolet transparent oxide, textured-dielectric coating for solar cells, and one-dimensional nanostructure forms for enhanced optical properties.[1–4] In this study, the Ga_2O_3 thin film with embedding Cr layer is demonstrated to exhibit resistive switching (RS) properties without electrical forming process, and is suitable for application in next-generation resistance random access memory (RRAM). The RRAM uses two distinguishable resistance states (low resistance state, which is ON state, and high resistance state, which is OFF state) to store digital data in a memory cell, and has the advantages of long data retention, low-power consumption, high-speed operation, high scalability, and simple fabrication procedures compatible with the standard CMOS process.[5,6]

However, a number of crucial issues must be solved, such as large operation parameters variation,[7–9] low device yield,[10] and high forming voltage.[11] A forming process is necessary to activate the resistive memory devices before performing any RS phenomenon. The forming process is a high-voltage stress applied on the pristine device, and the pristine device is subsequently changes from initial high resistance state (initial state) into ON state because of dielectric soft breakdown to generate point defects, such as oxygen vacancies at the anode.[11–15] The percolation of the oxygen vacancies moves toward the cathode under the high electric field. Consequently, the conducting path composed of oxygen vacancies is finally formed according to the analyzing results of x-ray absorption near-edge spectroscopy (XANES) and x-ray fluorescence (XRF) mapping.[12,13] The forming process is not only a time consuming process but also requires an extra high-voltage source in the memory circuit design. Removing the forming process can reduce time consumption and simplify the circuit design. Several methods were used to remove or suppress the forming voltage ($V_{forming}$) for the metal oxides, such as controlling the stoichiometry of the oxide,[5] reducing the film thickness,[6] and annealing the film at high temperature.[16]

The forming process is removed by embedding Cr metal layer in the middle of the Ga_2O_3 films with a rapid thermal annealing (RTA) in this study. The effects of the embedding Cr layer on the RS properties of the devices, and the related carrier conduction, are investigated to provide insight into the RS mechanism. The diffusion of Cr creates suitable amount of oxygen vacancies within the Ga_2O_3 films leading to forming-free RS behavior.

II. EXPERIMENTS

Before depositing an 80-nm-thick Pt bottom electrode, a 20-nm-thick Ti adhesion layer was deposited on SiO_2/Si substrate by electron beam evaporation. Subsequently, three sequential layers of Ga_2O_3/Cr/Ga_2O_3 with the thicknesses of 20/1.5/20 nm were deposited on Pt/Ti/SiO_2/Si substrates, where the Cr layer was fabricated by electron beam evaporation. The Ga_2O_3 films were deposited from a ceramic Ga_2O_3 target at 200 °C by a rf magnetron sputter, in which the base pressure of the sputtering chamber was below 2×10^{-5} Torr and the working pressure was 10 mTorr maintained by a gas mixture of oxygen and argon at a mixing ratio of 1:2 with a total flow of 18 sccm. Subsequently, the RTA was performed in N_2 ambient for 120 s at 500 (Cr-500), 600 (Cr-600) and 700 °C (Cr-700). Consequently, the Ga_2O_3-based devices with embedding Cr metal layer (Cr:Ga_2O_3) were completed. A 40 nm thick Ga_2O_3 film without embedding Cr metal layer was fabricated and RTA annealed at 600 °C for 120 s (N-600) as the reference sample. All of the Ga_2O_3 films with and without embedding Cr metal layer belong to β-phase with a preferred orientation of (400), as shown in Fig. 1(a), which was confirmed in previous studies.[17,18] It indicates that the embedding Cr layer has an ignoring influence on the

[a)]Electronic mail: tseng@cc.nctu.edu.tw.

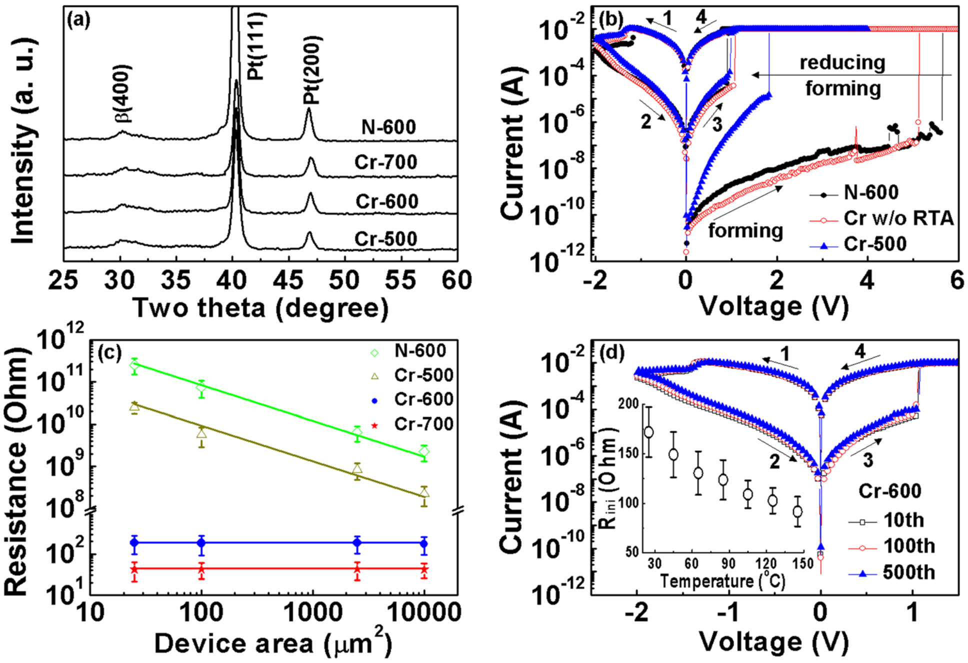

FIG. 1. (Color online) (a) XRD patterns of N-600, Cr-500, Cr-600, and Cr-700, respectively, in which the peaks exhibit a β-phase Ga_2O_3 with a preferred orientation of (400). (b) Typical RS $I-V$ curves of N-600 (solid circle), the $Ti/Cr:Ga_2O_3/Pt$ (empty circle) devices without RTA and Cr-500 (solid triangle), where the forming processes are also demonstrated. (c) The R_{ini} of N-600 and the $Ti/Cr:Ga_2O_3/Pt$ devices with various RTA temperatures vs device area. (d) 10th, 100th, and 500th $I-V$ curves of Cr-600 during continuous RS cycles at room temperature. The inset shows the R_{ini} vs temperature relationship for the Cr-600.

crystal structure of the Ga_2O_3 films. Finally, the areas of the Ti top electrode were patterned in the range from 25 to 10 000 μm^2 by the conventional photolithography and lift-off technique. Agilent 4155C semiconductor parameter analyzer was used to measure all of the current−voltage ($I-V$) curves in ambient atmosphere at room temperature. A two-probe configuration measurement in probe station was used. The bias voltage was applied on the Ti top electrode with the Pt bottom electrode grounded.

III. RESULTS AND DISCUSSION

Figure 1(b) depicts the typical $I-V$ curves of N-600, the $Ti/Cr:Ga_2O_3/Pt$ devices without RTA, and Cr-500. The operations of the bipolar RS cycle after a high-voltage forming process are represented by the arrows. The $V_{forming}$ of N-600 and the $Ti/Cr:Ga_2O_3/Pt$ without RTA devices are close, and are higher than that of Cr-500. The initial resistance (R_{ini}) of N-600 and the $Ti/Cr:Ga_2O_3/Pt$ without RTA is also relatively large as compared with those of both ON and OFF states. As RTA temperature is increased, the R_{ini} is lowered as shown in Fig. 1(c). The R_{ini} of N-600 and Cr-500 are considerably large and inverse to the areas of the device, and the forming process is required to reach ON state. However, an abrupt decrease in order of magnitude of the R_{ini} is demonstrated in Cr-600 and Cr-700. This low R_{ini} is equal to that of ON state and is nearly constant with reduced device area; hence, both devices become forming-free and the localized conducting filaments are expected to be formed after RTA.

The typical $I-V$ curve and successive RS operations of Cr-600 over 500 cycles are shown in Fig. 1(d), indicating the excellent RS endurance. Therefore, such a forming-free memory device is implemented by embedding a Cr layer with 600 °C RTA. The R_{ini} of Cr-600 decreases with increasing temperature, as shown in the inset of Fig. 1(d), which is semiconductor-like behavior. It suggests that the conducting filaments within Cr-600 are mainly composed of oxygen vacancies instead of Cr or Ga metals. No RS is observed for Cr-700 with the upper-limited current compliance (100 mA) in the Agilent 4155C. The film thickness effect on the $Cr:Ga_2O_3$ is also investigated, and the electrical properties of N-600 and the various thicknesses $Ti/Cr:Ga_2O_3/Pt$ devices with 600 °C RTA are summarized in Table I. A common forming process is required for N-600 and Cr-600L to trigger the RS in the memory devices; conversely, Cr-600 and Cr-600S are originally in ON state. The Cr-600 exhibits RS property, however, Cr-600S can not be switched back into OFF state, because of the high concentration of oxygen vacancies in the film. Consequently, the suitable concentration of oxygen vacancies has a considerable influence on the $Cr:Ga_2O_3$ film, resulting in the forming-free RS behaviors.

The Ga spectra are investigated by x-ray photoelectron spectrometer (XPS) to understand the bonding state of the embedding Cr within the Ga_2O_3 film. Figures 2(a)–2(d) show the Ga $2p_{2/3}$ spectra in the middle of the bulk layer. In contrast to N-600, the $Cr:Ga_2O_3$ films after RTA exhibit a metallic Ga $2p_{2/3}$ peak at 1116.9 eV, indicating that more oxygen vacancies are introduced within $Cr:Ga_2O_3$ films. The oxygen vacancies, associated with the formation of the conducting filaments, increase substantially when the RTA temperature is increased based on the intensity of metallic Ga $2p_{2/3}$ peak at 1116.9 eV. In Fig. 2(e), the position 2 is in the

TABLE I. A number of electrical characteristics of N-600 and the $Ti/Cr:Ga_2O_3/Pt$ devices with 600 °C RTA under various thicknesses.

	$Ga_2O_3/Cr/Ga_2O_3$ (nm)	Resistive Switching	$V_{forming}$ (V)	R_{ini} (Ohm)
N-600	40	Yes	5−7	~15 G
Cr-600S	10/1.5/10	N.A.	No	~50
Cr-600	20/1.5/20	Yes	No	~180
Cr-600L	40/1.5/40	Yes	2−3	1 G

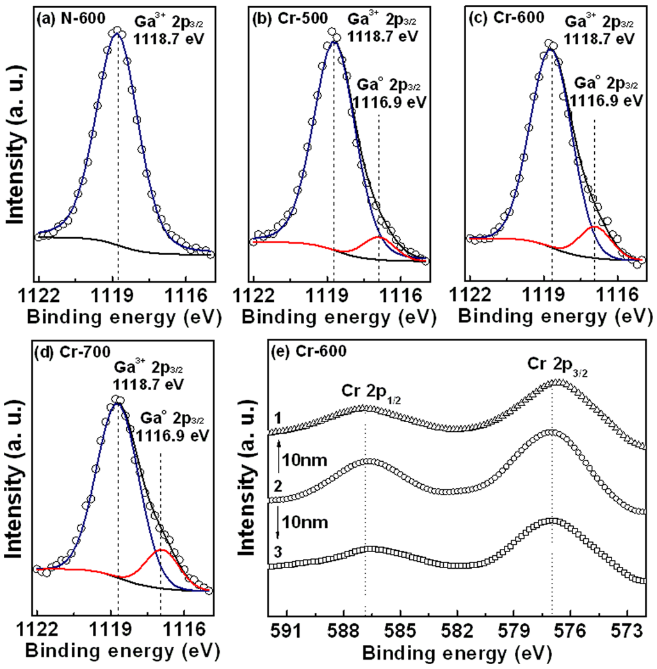

FIG. 2. (Color online) Ga $2p_{3/2}$ spectra of (a) N-600, (b) Cr-500, (c) Cr-600, and (d) Cr-700. (e) Cr $2p_{1/2}$ and Cr $2p_{3/2}$ in various positions (1, 2, and 3) within the Cr-600.

middle of Cr-600 film whereas the positions 1 and 3 are 10 nm above and below the position 2, respectively. The Cr $2p_{1/2}$ and Cr $2p_{3/2}$ peaks located at 586.8 and 577 eV, respectively, indicate that the embedding Cr diffuses and is oxidized to gain oxygen from Ga_2O_3 after RTA.[19] The Gibbs free energy of the Cr_2O_3 (-1058.1 kJ/mol) is lower than that of the Ga_2O_3 (-998.3 kJ/mol).[20] Therefore, point defects such as oxygen vacancies and metallic Ga are expected to be easily introduced within Cr-600 film by the Cr diffusion and oxidization. The embedding metal species, and the parameters of RTA, such as temperature and duration, as a result, could control the amount of oxygen vacancies in the Ga_2O_3 films.

The electrical forming process produces sufficient defects (especially oxygen vacancies) to form the localized conducting filaments to reach ON state.[12–15] For Cr-600 with forming-free RS behavior, the embedding Cr is expected to diffuse along the easily-diffused paths (such as grain boundaries) in the bulk during RTA and accompanies a suitable amount of oxygen vacancies created according to both results of the inset of Fig. 1(d) and Fig. 2. In addition, the Cr-600 exhibits the (400) preferred orientation [Fig. 1(a)]. The (400) oriented grains would form a columnar grain structure if they have nearly similar grain size.[21] This structure is favorable to provide the conducting filaments along grain boundaries. Moreover, the relation between the R_{ini} and the device area also indicates that the conducting filaments are locally formed along the grain boundaries. Conversely, the R_{ini} and the $V_{forming}$ of Cr-500 are reduced as compared with that without RTA. According to the XPS data [Figs. 2(b) and 2(c)], the concentration of oxygen vacancies within Cr-500 is lower than that within Cr-600. The Cr diffusion and oxidization in Cr-500 are considered more moderate at relatively low RTA temperature. The R_{ini} of Cr-500 ($\sim 10^9$ Ω) is larger than ON state resistance ($\sim$160 Ω) because it does not have sufficient oxygen vacancies to form the conducting filaments connected to the top and bottom electrodes. Therefore, the insufficient oxygen vacancies created in Cr-500 reduce its $V_{forming}$ as compared with that without RTA. The same phenomenon indicates that the forming process is required to achieve RS behavior of the thicker Cr-600L. However, the R_{ini} of Cr-700 ($\sim$60 Ω) is considerably lower than that of Cr-600 ($\sim$180 Ω). But, the Cr-700 does not exhibit RS behavior, because of the substantial oxygen vacancies created within it. A similar result is obtained for the $Cr:Ga_2O_3$ film with thinner thickness, such as Cr-600S with lower R_{ini} of 50 Ω. Therefore, only the film with a suitable amount of oxygen vacancies and columnar structure can exhibit forming-free RS behaviors.

Based on these results, the thermal-induced localized conducting filaments in the pristine Ti/$Cr:Ga_2O_3$/Pt is similar to those induced by electrical forming process. By controlling the RTA temperature and the $Cr:Ga_2O_3$ film thickness in this study, a suitable amount of point defects, such as oxygen vacancies, are created to compose the conducting filaments along the grain boundaries before performing RS cycle.

Recently, the electric faucet model was proposed in the metal-insulator-metal structure and at least one faucet was created at the high-resistance metal/insulator interface to regulate the current flow by switching itself on and off.[22] The oxide film bulk of the device exhibited high conductivity after the forming process, which was in series with the electric faucet at the interface. The considerable oxygen electromigration and the local chemical reaction at the relatively high-resistance interface were possible mechanisms for opening and closing of the electric faucet. It would have a similar conduction mechanism in N-600, the Ti/$Cr:Ga_2O_3$/Pt device without RTA, and Cr-600 devices, which demonstrated that the embedding Cr layer within Ga_2O_3 film with RTA modifies only the R_{ini} of $Cr:Ga_2O_3$ film by creating oxygen vacancies and forming the local conducting filaments. The opening and closing of the local faucets (created at the Ti/Ga_2O_3 interface) were controlled by the interfacial oxygen migration, causing the formation and rupture of the conducting filaments.[22]

The curve fittings are executed for both positive and negative bias regions of the $I-V$ characteristics in N-600, the Ti/$Cr:Ga_2O_3$/Pt device without RTA, and Cr-600 devices. Their respective double-logarithmic plots are shown in Figs. 3(a) and 3(b). The conduction mechanism in these three devices is consistent with space charge limit current (SCLC) theory.[23–25] In the low-voltage positive bias region, Ohmic conduction (slope = 1) is assumed to be caused by the thermal-free carriers exceeding the injected carriers, which is followed by the trap-unfilled SCLC (slope = 2). An abrupt current increase appears for the conducting filaments formation and trapping the injected charges. The second $I-V^2$ characteristics reappear in the positive bias region because the trapping centers are occupied by the injected carrier, creating a space charge region near the electrode and leading to an electric field to block further carrier injection (trap-filled SCLC). Finally, ON state is achieved and obeys the Ohmic

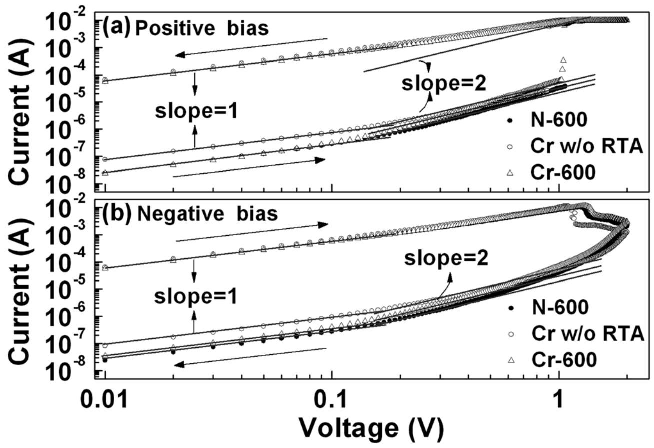

FIG. 3. $I-V$ characteristics of both (a) positive (b) negative bias regions of N-600, the Ti/Cr:Ga_2O_3/Pt without RTA, and Cr-600 devices plotted in a double-logarithmic scale.

conduction in the voltage-decreasing scan as shown in Fig. 3(a). In Fig. 3(b), the OFF process in the negative bias region, and the similar conduction mechanism, is observed, which obeys the SCLC theory with rupturing the conducting filaments near the interface close to Ti top electrode.[23] The embedding Cr layer within Ga_2O_3 film with RTA affects only the R_{ini} of Cr:Ga_2O_3 film by inducing oxygen vacancies. The interface between Ti and Cr:Ga_2O_3 film determines the switching mechanism.[25]

IV. CONCLUSIONS

The thermal-induced conducting filaments in the Ga_2O_3 films with Cr metal embedded are demonstrated in this study. With various RTA treatments, the Cr diffuses and is oxidized to some degree to cause the influences on the R_{ini} of Cr:Ga_2O_3 film. An increase of the concentration and relative distributions of the oxygen vacancies is obtained based on the XPS analyses. The forming-free RS behavior appears because the R_{ini} is equivalent to ON state. The carrier conduction mechanisms of the memory devices are efficiently explained by the trap-related SCLC theory. The embedding Cr layer within the Ga_2O_3 film with RTA modifies the R_{ini} of the film without influencing the RS mechanism. The interface between Ti and Cr:Ga_2O_3 film determines the RS mechanism. The proposed method provides an easy way to eliminate the forming process in the memory cell and, thus, the high-voltage source in the memory circuit design.

ACKNOWLEDGMENTS

This work was supported by the National Science Council, Taiwan, under project NSC 99-2221-E-009-166-MY3.

[1]M. Fleischer, W. Hanrieder, and H. Meixner, Thin Solid Films **190**, 93 (1990).
[2]M. Bartic, M. Ogita, M. Isai, C. L. Baban, and H. Suzuki, J. Appl. Phys. **102**, 023709 (2007).
[3]M. Rebien, W. Henrion, M. Hong, J. P. Mannaerts, and M. Fleischer, Appl. Phys. Lett. **81**, 250 (2002).
[4]R. Rao, A. M. Rao, B. Xu, J. Dong, S. Sharma, and M. K. Sunkara, J. Appl. Phys. **98**, 094312 (2005).
[5]I. G. Baek, M. S. Lee, S. Seo, M. J. Lee, D. H. Seo, D. S. Suh, J. C. Park, H. S. Kim, I. K. Yoo, U. I. Chung, and J. T. Moon, Tech. Dig.- Int. Electron Devices Meet. 587 (2004).
[6]H. Y. Lee, P. S. Chen, T. Y. Wu, Y. S. Chen, C. C. Wang, P. J. Tzeng, C. H. Lin, F. Chen, C. H. Lien, and M.-J. Tsai, Tech. Dig.- Int. Electron Devices Meet. 297 (2008).
[7]D. C. Kim, M. J. Lee, S. E. Ahn, S. Seo, J. C. Park, I. K. Yoo, J. G. Baek, H. J. Kim, E. Y. Yim, J. E. Lee, S. O. Park, H. S. Kim, U- In Chung, J. T. Moon, and B. I. Ryu, Appl. Phys. Lett. **88**, 232106 (2006).
[8]C. B. Lee, B. S. Kang, M. J. Lee, S. E. Ahn, G. Stefanovich, W. X. Xianyu, K. H. Kim, J. H. Hur, H. X. Yin, Y. Park, I. K. Yoo, J.-B. Park, and B. H. Park, Appl. Phys. Lett. **91**, 082104 (2007).
[9]C. Y. Lin, C. Y. Wu, C. Y. Wu, T. C. Lee, F. L. Yang, C. Hu, and T. Y. Tseng, IEEE Electron Device Lett. **28**, 366 (2007).
[10]D. Lee, D. Seong, H. Choi, I. Jo, R. Dong, W. Xiang, S. Oh, M. Pyun, S. Seo, S. Heo, M. Jo, D.-K. Hwang, H. K. Park, M. Chang, M. Hasan, and H. Hwang, Tech. Dig.- Int. Electron Devices Meet. 797 (2006).
[11]C. Y. Lin, D. Y. Lee, S. Y. Wang, C. C. Lin, and T. Y. Tseng, Surf. Coat. Technol. **203**, 628 (2008).
[12]M. Janousch, G. I. Meijer, U. Staub, B. Delley, S. F. Karg, and B. P. Andreasson, Adv. Mater. **19**, 2232 (2007).
[13]B. P. Andreasson, M. Janousch, U. Staub, and G. I. Meijer, Appl. Phys. Lett. **94**, 013513 (2009).
[14]R. E. Thurstans and D. P. Oxley, J. Phys. D **35**, 802 (2002).
[15]K. Kinoshita, T. Tamura, M. Aoki, Y. Sugiyama, and H. Tanaka, Appl. Phys. Lett. **89**, 103509 (2006).
[16]M. Kawai, K. Ito, N. Ichikawa, and Y. Shimakawa, Appl. Phys. Lett. **96**, 072106 (2010).
[17]T. Takeuchi, H. Ishikawa, N. Takeuchi, and Y. Horikoshi, Thin Solid Films **516**, 4593 (2008).
[18]F. K. Shan, G. X. Liu, W. J. Lee, G. H. Lee, I. S. Kim, and B. C. Shin, J. Appl. Phys. **98**, 023504 (2005).
[19]J. Chastain, *Handbook of X-ray Photoelectron Spectroscopy* Perkin-Elmer, Minnesota, 1992.
[20]*Handbook of Chemistry and Physics*, 84th ed., edited by D. R. Lide CRC Press, New York, 2003.
[21]M. H. Lin, M. C. Wu, Y. H. Huang, C. H. Lin, and T. Y. Tseng, IEEE Trans. Electron Devices **58**, 1182 (2011).
[22]I. H. Inoue, S. Yasuda, H. Akinaga, and H. Takagi, Phys. Rev. B **77**, 035105 (2008).
[23]C. Y. Lin, C. Y. Wu, C. Y. Wu, C. Hu, and T. Y. Tseng, J. Electrochem. Soc. **154**, G189 (2007).
[24]S. Kim, H. Y. Jeong, S. Y. Choi, and Y. K. Choi, Appl. Phys. Lett. **97**, 033508 (2010).
[25]D. Y. Lee, S. Y. Wang, and T. Y. Tseng, J. Electrochem. Soc. **157**, G166 (2010).